



1 **Atlantic Multidecadal Variability since 1850 is largely**
2 **externally forced**

3 Yongyao Liang¹, Ed Hawkins², Gerard McCarthy¹, Peter Thorne¹

4 ¹ Irish Climate Analysis and Research UnitS, Department of Geography, Maynooth
5 University, Co. Kildare, Ireland

6 ² National Centre for Atmospheric Science, Department of Meteorology, University of
7 Reading, Reading, United Kingdom

8 *Correspondence to:* Yongyao Liang (YONGYAO.LIANG.2025@mumail.ie)

9

10 **Abstract.** Whether observed Atlantic Multidecadal variability (AMV) is truly an intrinsic
11 internal mode of climate variability or an externally forced response remains
12 contentious, with conflicting literature that North Atlantic SST variability arises from
13 internal dynamics or external forcing. The availability of several single model initial-
14 condition large ensembles (SMILEs) and new insights into potential biases in sea
15 surface temperature (SST) variations offer a fresh opportunity to reassess this
16 question. We show that SMILE ensembles provide strong evidence that AMV-like
17 variability is largely externally forced. New insights into potential SST biases also raise
18 questions about apparent early 20th Century oscillatory behaviour. SMILE models with
19 stronger multidecadal variability show weaker agreement with observed AMV phasing,
20 even in the best performing individual ensemble members, suggesting that large
21 internal model variability may obscure the forced signal. We conclude that future
22 variations in North Atlantic SST will very likely be driven primarily by future
23 anthropogenic activities.



24 1 Introduction

25 AMV manifests as alternating warm and cold sea surface temperature (SST)
26 anomalies centred on the North Atlantic basin with a nominal cycle of 60 to 90 years
27 (Delworth and Mann, 2000). Such variations in North Atlantic SST (NASST) have been
28 linked to regional hydroclimate and surface temperature fluctuations over Europe and
29 North America (Sutton and Dong, 2012; Sutton and Hodson, 2005), and its influence
30 extends globally through teleconnections (Kravtsov et al., 2018). Despite its wide-
31 ranging relevance, the physical origin of AMV remains contested. There is ongoing
32 debate whether the observed NASST anomalies reflect a persistent internally
33 generated mode of climate variability, or a transient feature shaped by external forcing
34 (Bellomo et al., 2018; Booth et al., 2012; Clement et al., 2015; Klavans et al., 2022;
35 Knudsen et al., 2011; Murphy et al., 2017; Otterå et al., 2010).

36 One school of thought regards the AMV as an expression of naturally occurring internal
37 variability, typically associated with changes in the Atlantic Meridional Overturning
38 Circulation (AMOC) (Ba et al., 2014; Wang and Zhang, 2013; Wills et al., 2019; Zhang
39 et al., 2019) or stochastic atmospheric processes (Clement et al., 2015). From this
40 perspective, AMV phases are governed by natural dynamics and may be expected to
41 continue with a quasi-predictable pattern. In contrast, others argue that much of the
42 directly observed AMV signal is a coincidence that is preliminarily the response to
43 external drivers, particularly from anthropogenic GHGs and aerosol emissions
44 (Bellomo et al., 2018; Booth et al., 2012; Murphy et al., 2017) and volcanic activities
45 (Booth et al., 2012; Otterå et al., 2010). This distinction is critical: if the AMV is primarily
46 a natural oscillation, a transition to a cooling phase could be expected in the coming
47 decades; if externally forced, its future trajectory will largely follow the evolution of
48 external drivers, principally anthropogenic GHGs and aerosol emissions.

49 Resolving this debate is complex. First, the shortness and uncertainties of the
50 observational record potentially hinder robust detection of multidecadal oscillations
51 (Buckley and Marshall, 2016; Mann et al., 2020, 2021). Although reconstructions using
52 proxy data have identified multi-decadal variability in NASST extending back hundreds
53 or thousands of years (Gray et al., 2004; Knudsen et al., 2011), it is unclear whether
54 this is consistent with direct observations, and the interpretation of paleoclimate data
55 is challenged by proxy limitations and by difficulties in calibrating against a modern,



56 anthropogenically influenced climate (Mann et al., 2021). Second, the representation
57 of multidecadal variability in climate models is highly sensitive to model physics and
58 atmosphere-ocean coupling (Kravtsov et al., 2018; Wang and Zhang, 2013; Zhang et
59 al., 2019).

60 Internal variability is the natural fluctuations of the climate system that occur
61 independently of external factors. These variations stem from the inherent nonlinear
62 and chaotic nature of the atmosphere-ocean-ice-land system and are sensitive to
63 small differences in initial conditions (Lehner and Deser, 2023; Lorenz, 1963). In
64 climate modelling, internal variability is quantified by running multiple simulations with
65 identical external forcing but slightly different starting states. The divergence among
66 these simulations represents the range of plausible unforced climate outcomes.

67 Recent modelling innovations provide new tools for assessing the uncertainty
68 associated with internal variability. Single-model initial-condition large ensemble
69 simulations (SMILEs) have emerged as a powerful means of separating internal
70 variability from externally forced signals (Deser et al., 2020a, b). SMILE experiments
71 consist of multiple realisations from the same climate model, each with identical
72 external forcing but slightly perturbed initial conditions. This allows the model's internal
73 variability to emerge as the spread across ensemble members, while the ensemble
74 mean isolates the modelled forced response. Studies using SMILEs have shown that
75 ensemble means often evolve in phase with observed AMV signals, lending support
76 to the argument that AMV signals may be externally forced (Bellomo et al., 2018; Booth
77 et al., 2012; Murphy et al., 2017). However, others highlight the persistence of
78 internally generated variability, particularly in the latter half of the 20th century (Kim et
79 al., 2018). High-resolution climate models offer another way to study the internal
80 atmospheric and oceanic dynamics, and have also successfully replicated AMV-like
81 patterns (Hao et al., 2025).

82 This study is focused on an ensemble-based separation of AMV signals by
83 incorporating seven SMILEs and a 52-member ensemble of historical runs from
84 CMIP6 models to quantify the forced components and the internal variability envelope
85 of North Atlantic multidecadal SST variability over the period 1850-2014.



86 2 Data and Method

87 2.1 Observational datasets and model simulations

88 Three SST observations are used: DCENT (Chan et al., 2024), HadSST4 (Kennedy
89 et al., 2019) and ERSST5 (Huang et al., 2026). Historical simulations come from seven
90 SMILEs produced by six modelling centres (Supplementary Table 1), each SMILE run
91 within the same model with small perturbations introduced to either their initial
92 atmospheric or ocean conditions; some models perturb both. Alongside, a multimodel
93 ensemble is formed by using the first realisation (r1i1p1f1) from the 52 CMIP6 models
94 that were available through the UK Science and Technology Facilities Council (STFC)
95 Centre for Environmental Data analysis (CEDA) Archive at the time of analysis
96 (Supplementary Table 2). The historical forcing followed a prescribed CMIP5 forcing
97 (Taylor et al., 2012) for MPI-GE and CESM1-LENS, and a CMIP6 forcing (Eyring et
98 al., 2016) for the remaining LEs. Most simulations span 1850 to 2014, however, shorter
99 coverage SMILEs such as MPI-GE, CESM1-LENS and CANARI are retained in the
100 analysis to broaden model physics sampling and strengthen ensemble-based
101 conclusions.

102 2.2 AMV indices

103 The computation of AMV indices follows a consistent methodology applied to both
104 observational and simulation data, following (Barghorn et al., 2025; Robson et al.,
105 2023). Monthly SST anomalies were rebased to a common 1961-1990 climatology,
106 then averaged into annual means. All grid cell data were bilinearly interpolated to
107 regrid onto a 5×5 resolution consistent with the HadSST4 grid. Due to the consistent
108 data availability across the North Atlantic domain during the study period, masking to
109 match HadSST4 or DCENT spatiotemporal coverage was deemed unnecessary.
110 Annual anomalies for the North Atlantic region ($0-60^\circ$ N, $0-80^\circ$ W) were extracted and
111 aggregated into an area-weighted mean timeseries. A best-fit linear trend over the
112 entire timeseries for each large ensemble was removed to eliminate the long-term
113 warming trend. Last, the series were smoothed with a centred 10-year rolling average.



114 Methodological choices used to remove long-term warming trends have a direct
115 influence on the inferred AMV index (Frankcombe et al., 2018; Peings et al., 2016;
116 Robson et al., 2023; Si and Hu, 2017a). To assess sensitivity, AMV indices were
117 recalculated using detrending methods: linear detrending of NASST timeseries, as in
118 the main text; and a second-order polynomial fit detrending of NASST times series.
119 Only the detrending methods vary, the other procedures follow the same exact steps.

120 For each large ensemble (LE), the mean across the ensemble members is taken as
121 the forced response, since averaging cancels random internally generated variability
122 while preserving the common response to external forcing.

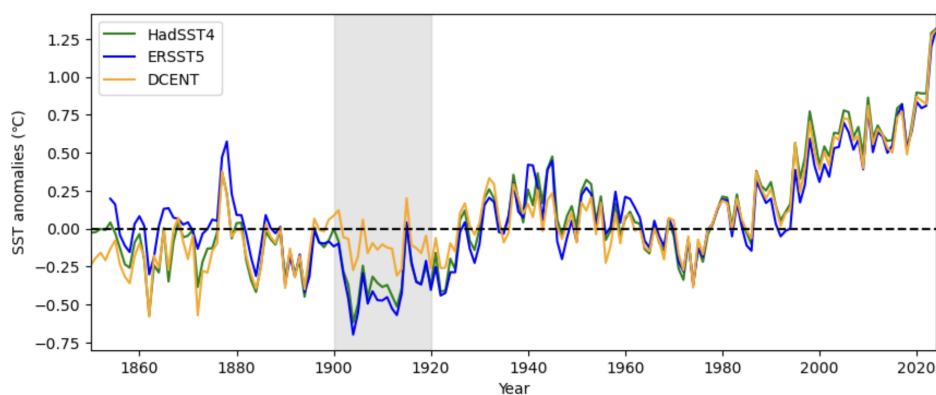


123 3 Results

124 3.1 Sea surface temperature uncertainties

125 Differences between historical SST estimates can complicate AMV diagnosis. A
126 critical example of SST observation uncertainty is a possible early twentieth-century
127 cold bias (Sippel et al., 2024), which has been recently reevaluated and adjusted in
128 the Dynamically Consistent ENsemble of Temperature (DCENT) dataset (Chan et al.,
129 2024). Between 1900-1920, DCENT exhibits systematically higher NASST anomalies
130 compared to the two most widely used records, HadSST4 and NOAA ERSST5,
131 substantially modifying apparent multidecadal variability (Fig. 1). Given these inter-
132 dataset differences, the subsequent analysis adopts two SST datasets: HadSST4,
133 which reflects the conventional records; and DCENT which reflects the new insights
134 into early 20th Century NASSTs. Using both datasets enables a more comprehensive
135 assessment of model-observation comparisons and reduces the risk of over-reliance
136 on a single, potentially biased observational estimate.

137



138

139 Figure 1 Observed annual SST anomalies over the North Atlantic domain (0-60°N, 0-
140 80°W), relative to the 1961-1990 average, HadSST4 (green), ERSST5 (blue) and
141 DCENT (orange). The grey-shaded area represents the period of maximum
142 divergence between the three SST estimates.



143 3.2 Ensemble means track AMV phase

144 The SMILE ensemble results fall into two distinct categories. Several SMILE models
145 exhibit limited multidecadal variability in their ensembles whereas others exhibit
146 substantial multidecadal variability. In CESM2-LENS2, taken as an example of the first
147 family which exhibit limited multidecadal variability, the ensemble mean closely tracks
148 the observed AMV evolution ($R^2=0.84$ with HadSST4, $R^2=0.93$ with DCENT), and the
149 individual ensemble members display similar phase transitions (the average member-
150 observation-correlation is 0.73 with HadSST4 and 0.81 with DCENT) (Fig. 2a),
151 including early twentieth-century cooling, a 1930-1950 warm phase, the mid-century
152 cooling and post-1970 warming. The ensemble mean falls within the range defined by
153 the two observational datasets, except during the 1930-50 warming, which appears to
154 be damped in the model. This close alignment between the ensemble mean, individual
155 members and observations suggests that in CESM2-LENS2, the AMV-like oscillations
156 are primarily externally forced. This externally forced AMV-like behaviour is not
157 exclusive to CESM2-LENS2, similar consistency with observations is found in several
158 other SMILEs that exhibit intrinsically limited multidecadal ensemble variability
159 (CESM1-LENS, CanESM5-LE, MIROC-LE and CANARI-LE; Supplementary Fig. 1-4).
160 If the AMV were an expression of internal variability, such coherent multidecadal
161 features would not be visible: the ensemble members would evolve more
162 independently, and by averaging across the ensemble members, the internal
163 variability would cancel on averaging, yielding a comparatively flat ensemble mean.

164 By contrast, FGOALS-LE which in its SMILE ensemble has large multidecadal
165 variability, exhibits a relatively flat ensemble mean, and a wide spread amongst
166 ensemble members (Fig. 2b). The overall agreement with observations ($R^2=0.79$ with
167 HadSST4, $R^2=0.65$ with DCENT) is considerably lower than in CESM2-LENS2, the
168 average member-observation-correlation (grey dashed line) is also systematically
169 lower than the ensemble-mean-observations correlation (blue dashed line). The
170 presence of substantial decadal variability means that FGOALS-LE struggles to
171 replicate observed behaviour. A comparable behaviour is evident in the other SMILE
172 with large multidecadal internal variability (MPI-GE, Supplementary Fig. 5).

173 The ensemble members within each SMILE that maximised correlation with each
174 observational series were identified. Again, CESM2-LENS2 ensemble members show



175 a greater similarity with observations compared to those from FGOALS-LE (Figure 2).
176 This behaviour holds across other models as well; models with lower intrinsic
177 multidecadal variability consistently perform better in replicating observed AMV
178 behaviour (Supplementary Fig. 1-5). If AMV were internally generated then it would be
179 expected that while on average a model which captured the relevant physics might not
180 capture the observed signal well, when run enough times in a SMILE context it would,
181 by chance, have a member that was in phase and better reproduced the observed
182 behaviour. This is not the case for either FGOALS-LE or MPI-GE. Their best ensemble
183 member is less well correlated than that for the models with small intrinsic multidecadal
184 NASST variability.

185 In CESM2-LENS2 (Fig. 2a), no individual ensemble member reproduces the
186 pronounced cooling around 1910 as seen in HadSST4. Previous studies have
187 interpreted such mismatches as model limitations in reproducing the multidecadal
188 variability, especially for the twentieth century (Kravtsov et al., 2018). However, after
189 applying their bias correction to early twentieth-century SST records, the DCENT
190 dataset shows a greater agreement with the CESM2 ensemble mean during 1910-
191 1930 (RMSE=0.05°C) than HadSST4 (RMSE=0.16°C). This suggests that a large part
192 of the apparent discrepancy could arise from observational biases rather than model
193 errors. This would also add credence to recent findings (Sippel et al., 2024) suggesting
194 that DCENT may more faithfully reflect the physically consistent evolution of NASST
195 anomalies over this interval.

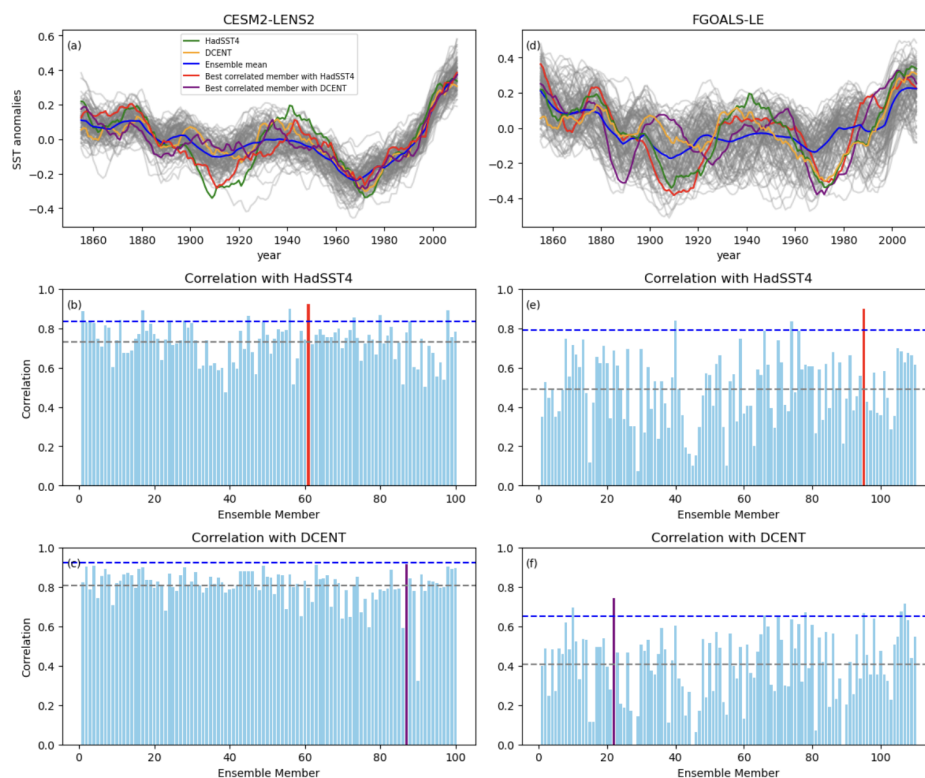


Figure 2 AMV indices and correlation statistics from CISM2-LENS2 (left) and FGOALS-LE (right) over 1855-2010. **a**, AMV indices from CISM2-LENS2, calculated by linear detrending the annual average NASST and smoothed with a 10-year rolling mean. The forced signal is represented by an ensemble mean (blue). Comparison is made with observed AMV derived from HadSST4 (green) and DCENT (orange). The ensemble member that is best correlated with the HadSST4 (red) and DCENT (purple) is also highlighted. **b**, correlation coefficient between each CISM2-LENS2 member and HadSST4. The ensemble mean correlation is shown with a blue dashed line, the average correlation across members is shown with a grey dashed line. **c**, Same as **b**, but for correlation with DCENT. **d-f**, same as **a-c**, respectively, but for FGOALS-LE.



197 Given the contrasting AMV-like behaviour in different SMILEs, we further examine the
198 model-dependent AMV-pattern by including the first historical simulation (r1i1p1f1)
199 from those models participating in CMIP6 that were available via the UK STFC node
200 and treating them collectively as a pseudo-SMILE. Unlike SMILEs, which isolate
201 internal variability within a single model structure, this multi-model approach
202 introduces structural model uncertainty, encompassing different physical
203 parameterisations and ocean-atmosphere coupling schemes.

204 The spread in SST anomalies across the CMIP6 ensemble is considerably larger than
205 in any single-model large ensemble, reflecting the combination of model uncertainty
206 and internal variability (Fig. 3). Despite this, the CMIP6 multi-model mean captures the
207 phasing of key multidecadal features evident in the observational records, though, the
208 1930-1950 warming phase remains damped, as in the SMILEs. The best
209 observations-matched members closely follow the observations, as in CESM2-LENS2
210 (Fig. 2a-c).

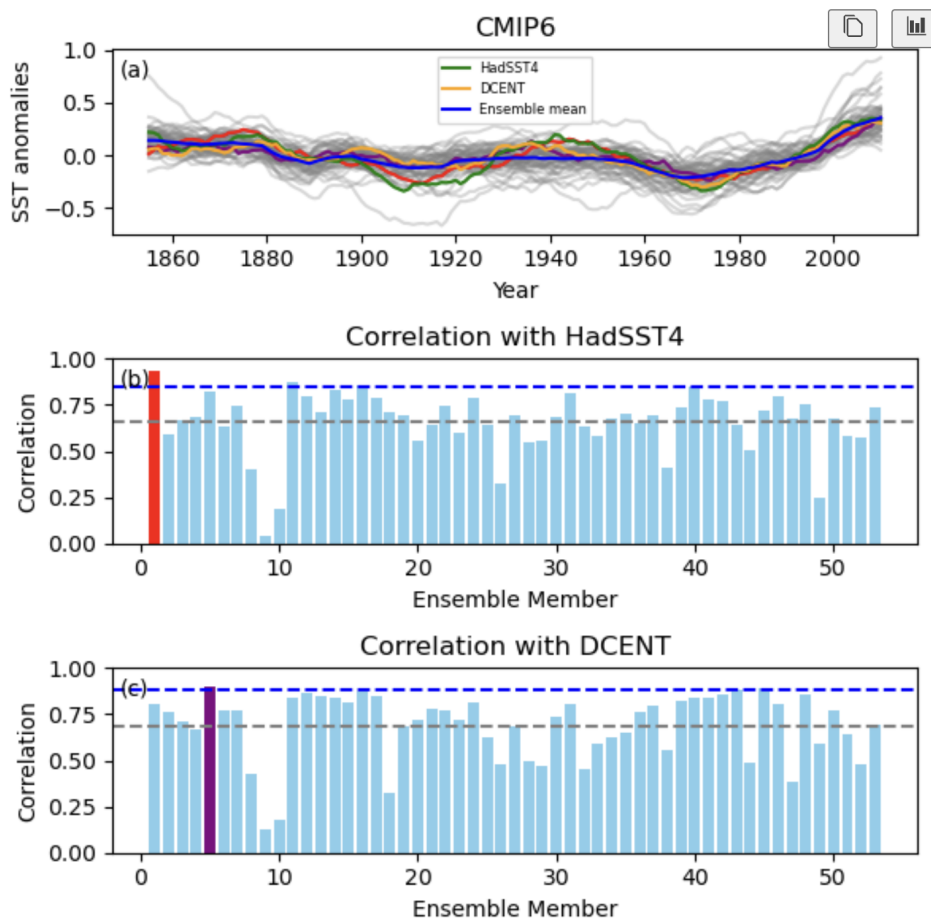


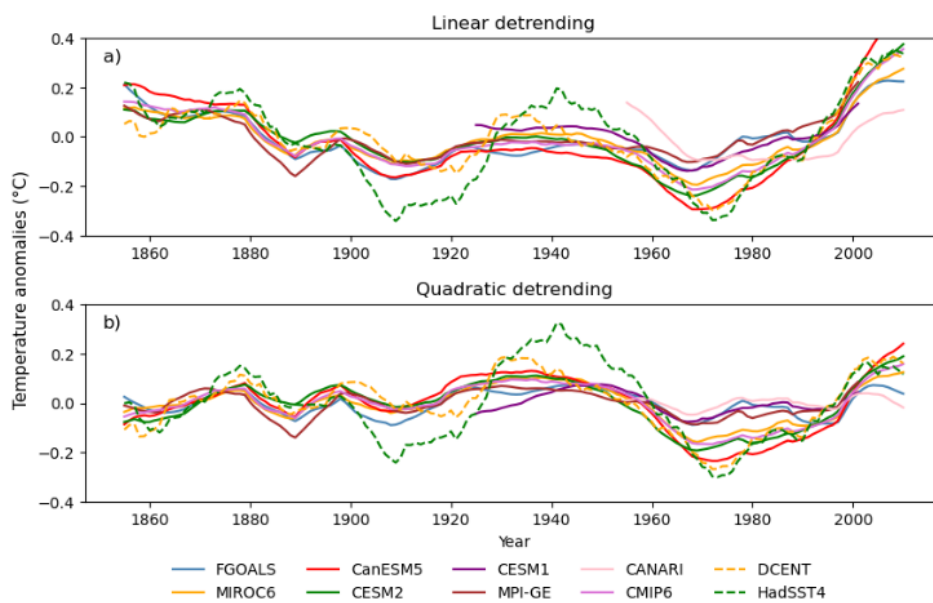
Figure 3 AMV indices from the first simulation of 52 models in CMIP6. The multi-model ensemble mean is shown in blue. Observational datasets include HadSST4 (green) and DCENT (orange). Same as Fig. 2, but for CMIP6 models.



211 Overall, the ensemble means from seven SMILEs and the CMIP6 ensemble broadly
212 tracked the observed AMV behaviour (Fig. 4a). Several robust inferences can be
213 drawn. First, the phasing of AMV is highly consistent across models and observations,
214 with most ensemble means capturing the major multidecadal transitions. Second, the
215 amplitude of these swings is systematically weaker in most ensemble means relative
216 to HadSST4 and to a much lesser extent DCENT, especially the nearly flat 1930-1950
217 warm phase, a feature that recurs across many SMILEs and in the CMIP6 mean. This
218 might be associated with a potential warm bias during World War II (Chan and
219 Huybers, 2021) which remains unresolved. Third, none of the ensemble means
220 reproduces the ~1910 cooling evident in HadSST4, instead, the ensemble means
221 cluster more closely around DCENT during this interval. Taken together, the alignment
222 in timing of AMV phase transitions across these structurally diverse models, despite
223 differences in internal variability, robustly implies the presence of a common forced
224 signal governing NASST variability over the entire observational record and heavily
225 discounts the potential that it arises from internal multidecadal variability. The better
226 agreement with DCENT also highlights the likelihood of residual biases in both
227 HadSST4 and ERSSTv5 in the early 20th Century, at least in the North Atlantic basin.

228 3.3 Sensitivity analysis to detrending method

229 The two detrending approaches captured the principal AMV features from the
230 observational records (Fig. 4), with the timing of the phase transitions largely
231 unchanged, but the amplitude varies substantially. Linear detrending yields a stronger
232 magnitude, particularly exaggerating the mid-20 century warming in HadSST4. The
233 ensemble mean from linear and quadratic detrending, yields similar inferred variability.
234 Consistent with previous findings (Si and Hu, 2017b), the phase transitions are robust
235 to methodological choices, whereas amplitude is more sensitive.



236

237 Figure 4 Sensitivity of AMV index to detrending methods. a, AMV indices derived
238 from linear detrending of NASST, compared with HadSST4 (green dashed line) and
239 DCENT (orange dashed line). b, same as a, using quadratic detrending.



240 4 Summary and Discussion

241 The physical causes of AMV remain disputed (Robson et al., 2023). Ensemble means
242 from SMILE simulations reproduce the observed AMV temporal evolution under
243 prescribed external forcing, particularly for those models with limited intrinsic
244 multidecadal variability, indicating that AMV-like variability is predominantly a forced
245 response. Our analysis thus supports the growing evidence that external forcing, such
246 as by anthropogenic emissions and volcanic effects, exerts a dominant influence on
247 multidecadal NASST variability (Bellomo et al., 2018; Booth et al., 2012; Klavans et
248 al., 2022; Murphy et al., 2017). Thus, the future trajectory of NASST and the nearby
249 continents' climate will largely evolve as a result of future emission choices.

250 A counterintuitive result emerges when comparing SMILEs. Models with stronger
251 multidecadal variability, such as FGOALS-LE (Fig. 2d) and MPI-GE (Supplementary
252 Fig. 5), perform less well in replicating the observed AMV evolution. While such models
253 might be expected to better capture observed variability through their internal
254 dynamics representation, correlation analysis reveals that even the best-correlated
255 ensemble members in these models deviate more from the observed AMV than those
256 from models with weaker multidecadal variability, such as CESM2-LENS2 (Fig. 2a) or
257 MIROC6-LE (Supplementary Fig. 2). This raises a critical question: could strong
258 multidecadal internal variability be actively unhelpful for capturing observed AMV
259 features? One possibility is that in models where internal variability dominates,
260 ensemble members evolve too independently, masking the externally forced signal
261 that governs observed phase transitions. Conversely, in models where internal
262 variability is more subdued, the forced signal is more distinct.

263 Discrepancies between observations and projections can be traced to several factors.
264 First, internal variability explains part of the residual, as observed trajectories often lie
265 within the ensemble spread. Second, anthropogenic aerosols can modulate the ocean
266 dynamics by strengthening AMOC, they enhance northward heat transport and
267 partially offsets the initial cooling (Robson et al., 2022). In the context of AMV, the
268 magnitude of externally forced SST variation may be muted by AMOC variability.
269 Third, observational uncertainty can introduce systematic errors in estimating
270 variability amplitude. From the possible cold biases in the early 20th century (Sippel
271 et al., 2024), to the unresolved World War II warm anomaly (Chan and Huybers, 2021),



272 the reliability of SST records is often overlooked and too quickly attributed to internal
273 variability, and thus warrants more attention (Folland et al., 2018; Osborn and
274 Kennedy, 2024). Fourth, model design limitations, particularly the inability to reproduce
275 the magnitude and spatiotemporal structure of observed multidecadal variability
276 (Kravtsov et al., 2018; Zhang et al., 2019), together with initialization choices
277 contribute to systematic biases. Recent work shows that simulations initialised from
278 1750 improved representation of earlier 20th century cooling (Ballinger et al., 2026).
279 Last, the prescribed volcanic forcing may itself be underestimated, numerous studies
280 indicate that CMIP5 and CMIP6 forcing datasets have overlooked the volcanic forcing
281 in both the future and historical periods (Bethke et al., 2017; Chim et al., 2025).

282 Interpretation of AMV-like variability is sensitive to AMV index calculation. The
283 common approach to isolate global-scale warming is linear detrending of NASST
284 (Bellomo et al., 2018; Huang et al., 2021; Si and Hu, 2017a), however, it often
285 overestimates the AMV amplitude (Robson et al., 2023). Regression-based
286 approaches using global mean SST can remove part of the genuine AMV variability,
287 leading to underestimation (Peings et al., 2016). Several studies have concluded that
288 the inferred external responses are highly dependent on the methodological choices,
289 as well as the time periods considered (Christiansen et al., 2025; Robson et al., 2023).
290 Despite these differences, the essential phase transitions and low-frequency variability
291 remain robust (Si and Hu, 2017a). A comparison of the sensitivity of our principal
292 findings to different detrending methods is provided and shown unaffected by such
293 choices.

294 Future work could extend the attribution of forced responses by separating individual
295 anthropogenic drivers, an approach that is becoming increasingly feasible with the
296 growing availability of single forcing simulations. Recent applications of single forcing
297 large ensemble have demonstrated their potential for attributing AMV (Huang et al.,
298 2021) and the updated CESM2 single forcing large ensemble (Simpson et al., 2023)
299 provides longer simulations and improved model design, offering new opportunities for
300 more robust attribution analyses.



301 Data availability

302 The observational sea surface temperature DCENT (Chan et al., 2024) is available
303 at <https://climatedataguide.ucar.edu/climate-data/dcent>; HadSST4 (Kennedy et al.,
304 2019) is available at <https://climatedataguide.ucar.edu/climate-data/sst-data-hadsst4>;
305 and ERSST5(NOAA Extended Reconstructed Sea Surface Temperature (ERSST),
306 Version 5, 2026) is available at
307 <https://psl.noaa.gov/data/gridded/data.noaa.ersst.v5.html>.

308 The modelling outputs of MPI-GE (Maher et al., 2019) is available at [https://esgf-](https://esgf-metagrid.cloud.dkrz.de/datacart/add_all/1/4779/?back=/search_reload/)
309 [metagrid.cloud.dkrz.de/datacart/add_all/1/4779/?back=/search_reload/](https://esgf-metagrid.cloud.dkrz.de/datacart/add_all/1/4779/?back=/search_reload/); CESM1-
310 LENS1 (Kay et al., 2015) [https://www.cesm.ucar.edu/community-projects/lens/data-](https://www.cesm.ucar.edu/community-projects/lens/datasets)
311 [sets](https://www.cesm.ucar.edu/community-projects/lens/datasets); CESM2-LENS2 (Rodgers et al., 2021)
312 <https://gdex.ucar.edu/datasets/d651056/>; FGOALS super LE (Zhao, 2023)
313 <https://www.scidb.cn/en/detail?dataSetId=f75af1c5d2cf484faa354437dc85acfc>.
314 CANARI-LE (Williams et al., 2018), MIROC6-LE(Shiogama et al., 2023) and
315 CanESM5-LE (Swart et al., 2019), CMIP6 multi-model ensemble is achieved at the
316 UK Science and Technology Facilities Council Centre for Environmental Data
317 Analysis (CEDA).

318

319 Code availability

320 Analysis scripts used for this study are available at
321 https://github.com/YongyaoLiang/AMV_LE_simulations



322 References

- 323 Ba, J., Keenlyside, N. S., Latif, M., Park, W., Ding, H., Lohmann, K., Mignot, J.,
324 Menary, M., Otterå, O. H., Wouters, B., Salas y Melia, D., Oka, A., Bellucci, A., and
325 Volodin, E.: A multi-model comparison of Atlantic multidecadal variability, *Clim. Dyn.*,
326 43, 2333–2348, <https://doi.org/10.1007/s00382-014-2056-1>, 2014.
- 327 Ballinger, A. P., Schurer, A. P., Hegerl, G. C., Dittus, A. J., Hawkins, E., Cornes, R.,
328 Kent, E. C., Marshall, L. R., Morice, C. P., Osborn, T. J., Rayner, N. A., and Rumbold,
329 S. T.: Importance of beginning industrial-era climate simulations in the eighteenth
330 century, *Environ. Res. Lett.*, 21, 014022, <https://doi.org/10.1088/1748-9326/ae1bbc>,
331 2026.
- 332 Barghorn, L., Börgel, F., Gröger, M., and Meier, H. E. M.: Atlantic multidecadal
333 variability control on European sea surface temperatures is mainly externally forced,
334 *Environ. Res. Lett.*, 20, 034044, <https://doi.org/10.1088/1748-9326/adb6bf>, 2025.
- 335 Bellomo, K., Murphy, L. N., Cane, M. A., Clement, A. C., and Polvani, L. M.: Historical
336 forcings as main drivers of the Atlantic multidecadal variability in the CESM large
337 ensemble, *Clim. Dyn.*, 50, 3687–3698, <https://doi.org/10.1007/s00382-017-3834-3>,
338 2018.
- 339 Bethke, I., Outten, S., Otterå, O. H., Hawkins, E., Wagner, S., Sigl, M., and Thorne,
340 P.: Potential volcanic impacts on future climate variability, *Nat. Clim. Change*, 7, 799–
341 805, <https://doi.org/10.1038/nclimate3394>, 2017.
- 342 Booth, B. B. B., Dunstone, N. J., Halloran, P. R., Andrews, T., and Bellouin, N.:
343 Aerosols implicated as a prime driver of twentieth-century North Atlantic climate
344 variability, *Nature*, 484, 228–232, <https://doi.org/10.1038/nature10946>, 2012.
- 345 Buckley, M. W. and Marshall, J.: Observations, inferences, and mechanisms of the
346 Atlantic Meridional Overturning Circulation: A review, *Rev. Geophys.*, 54, 5–63,
347 <https://doi.org/10.1002/2015RG000493>, 2016.
- 348 Chan, D. and Huybers, P.: Correcting Observational Biases in Sea Surface
349 Temperature Observations Removes Anomalous Warmth during World War II, *J.*
350 *Clim.*, 34, 4585–4602, <https://doi.org/10.1175/JCLI-D-20-0907.1>, 2021.
- 351 Chan, D., Gebbie, G., Huybers, P., and Kent, E. C.: A Dynamically Consistent
352 ENsemble of Temperature at the Earth surface since 1850 from the DCENT dataset,
353 *Sci. Data*, 11, 953, <https://doi.org/10.1038/s41597-024-03742-x>, 2024.
- 354 Chim, M. M., Aubry, T. J., Smith, C., and Schmidt, A.: Neglecting future sporadic
355 volcanic eruptions underestimates climate uncertainty, *Commun. Earth Environ.*, 6, 1–
356 10, <https://doi.org/10.1038/s43247-025-02208-1>, 2025.
- 357 Christiansen, B., Yang, S., and Drews, A.: The Atlantic Multidecadal Variability in
358 Observations and in a Large Historical Multimodel Ensemble: Forced and Internal
359 Variability, *J. Clim.*, 38, 2761–2781, <https://doi.org/10.1175/JCLI-D-24-0310.1>, 2025.



- 360 Clement, A., Bellomo, K., Murphy, L. N., Cane, M. A., Mauritsen, T., Rädel, G., and
361 Stevens, B.: The Atlantic Multidecadal Oscillation without a role for ocean circulation,
362 *Science*, 350, 320–324, <https://doi.org/10.1126/science.aab3980>, 2015.
- 363 Delworth, T. L. and Mann, M. E.: Observed and simulated multidecadal variability in
364 the Northern Hemisphere, *Clim. Dyn.*, 16, 661–676,
365 <https://doi.org/10.1007/s003820000075>, 2000.
- 366 Deser, C., Lehner, F., Rodgers, K. B., Ault, T., Delworth, T. L., DiNezio, P. N., Fiore,
367 A., Frankignoul, C., Fyfe, J. C., Horton, D. E., Kay, J. E., Knutti, R., Lovenduski, N. S.,
368 Marotzke, J., McKinnon, K. A., Minobe, S., Randerson, J., Screen, J. A., Simpson, I.
369 R., and Ting, M.: Insights from Earth system model initial-condition large ensembles
370 and future prospects, *Nat. Clim. Change*, 10, 277–286,
371 <https://doi.org/10.1038/s41558-020-0731-2>, 2020a.
- 372 Deser, C., Phillips, A. S., Simpson, I. R., Rosenbloom, N., Coleman, D., Lehner, F.,
373 Pendergrass, A. G., DiNezio, P., and Stevenson, S.: Isolating the Evolving
374 Contributions of Anthropogenic Aerosols and Greenhouse Gases: A New CESM1
375 Large Ensemble Community Resource, *J. Clim.*, 33, 7835–7858,
376 <https://doi.org/10.1175/jcli-d-20-0123.1>, 2020b.
- 377 Eyring, V., Bony, S., Meehl, G. A., Senior, C. A., Stevens, B., Stouffer, R. J., and
378 Taylor, K. E.: Overview of the Coupled Model Intercomparison Project Phase 6
379 (CMIP6) experimental design and organization, *Geosci. Model Dev.*, 9, 1937–1958,
380 <https://doi.org/10.5194/gmd-9-1937-2016>, 2016.
- 381 Folland, C. K., Boucher, O., Colman, A., and Parker, D. E.: Causes of irregularities in
382 trends of global mean surface temperature since the late 19th century, *Sci. Adv.*, 4,
383 [eaa05297](https://doi.org/10.1126/sciadv.aao5297), <https://doi.org/10.1126/sciadv.aao5297>, 2018.
- 384 Frankcombe, L. M., England, M. H., Kajtar, J. B., Mann, M. E., and Steinman, B. A.:
385 On the Choice of Ensemble Mean for Estimating the Forced Signal in the Presence of
386 Internal Variability, *J. Clim.*, 31, 5681–5693, <https://doi.org/10.1175/JCLI-D-17-0662.1>, 2018.
- 388 Gray, S. T., Graumlich, L. J., Betancourt, J. L., and Pederson, G. T.: A tree-ring based
389 reconstruction of the Atlantic Multidecadal Oscillation since 1567 A.D., *Geophys. Res.
390 Lett.*, 31, <https://doi.org/10.1029/2004GL019932>, 2004.
- 391 Hao, X., Sein, D. V., Spiegl, T., Niu, L., Chen, X., and Lohmann, G.: Modeling the
392 Atlantic Multidecadal Oscillation: The High-Resolution Ocean Brings the Timescale;
393 the Atmosphere, the Amplitude, *Ocean-Land-Atmosphere Res.*, 4, 0085,
394 <https://doi.org/10.34133/olar.0085>, 2025.
- 395 NOAA Extended Reconstructed Sea Surface Temperature (ERSST), Version 5:
396 [https://www.ncei.noaa.gov/access/metadata/landing-](https://www.ncei.noaa.gov/access/metadata/landing-page/bin/iso?id=gov.noaa.ncdc:C00927)
397 [page/bin/iso?id=gov.noaa.ncdc:C00927](https://www.ncei.noaa.gov/access/metadata/landing-page/bin/iso?id=gov.noaa.ncdc:C00927), last access: 20 January 2026.
- 398 Huang, H., Patricola, C. M., Winter, J. M., Osterberg, E. C., and Mankin, J. S.: Rise in
399 Northeast US extreme precipitation caused by Atlantic variability and climate change,



- 400 Weather Clim. Extrem., 33, 100351, <https://doi.org/10.1016/j.wace.2021.100351>,
401 2021.
- 402 Kay, J. E., Deser, C., Phillips, A., Mai, A., Hannay, C., Strand, G., Arblaster, J. M.,
403 Bates, S. C., Danabasoglu, G., Edwards, J., Holland, M., Kushner, P., Lamarque, J.-
404 F., Lawrence, D., Lindsay, K., Middleton, A., Munoz, E., Neale, R., Oleson, K., Polvani,
405 L., and Vertenstein, M.: The Community Earth System Model (CESM) Large Ensemble
406 Project: A Community Resource for Studying Climate Change in the Presence of
407 Internal Climate Variability, <https://doi.org/10.1175/BAMS-D-13-00255.1>, 2015.
- 408 Kennedy, J. J., Rayner, N. A., Atkinson, C. P., and Killick, R. E.: An Ensemble Data
409 Set of Sea Surface Temperature Change From 1850: The Met Office Hadley Centre
410 HadSST.4.0.0.0 Data Set, *J. Geophys. Res. Atmospheres*, 124, 7719–7763,
411 <https://doi.org/10.1029/2018JD029867>, 2019.
- 412 Kim, W. M., Yeager, S. G., and Danabasoglu, G.: Key Role of Internal Ocean
413 Dynamics in Atlantic Multidecadal Variability During the Last Half Century, *Geophys.*
414 *Res. Lett.*, 45, 13,449–13,457, <https://doi.org/10.1029/2018GL080474>, 2018.
- 415 Klavans, J. M., Clement, A. C., Cane, M. A., and Murphy, L. N.: The Evolving Role of
416 External Forcing in North Atlantic SST Variability over the Last Millennium, *J. Clim.*,
417 35, 2741–2754, <https://doi.org/10.1175/JCLI-D-21-0338.1>, 2022.
- 418 Knudsen, M. F., Seidenkrantz, M.-S., Jacobsen, B. H., and Kuijpers, A.: Tracking the
419 Atlantic Multidecadal Oscillation through the last 8,000 years, *Nat. Commun.*, 2, 178,
420 <https://doi.org/10.1038/ncomms1186>, 2011.
- 421 Kravtsov, S., Grimm, C., and Gu, S.: Global-scale multidecadal variability missing in
422 state-of-the-art climate models, *Npj Clim. Atmospheric Sci.*, 1, 34,
423 <https://doi.org/10.1038/s41612-018-0044-6>, 2018.
- 424 Lehner, F. and Deser, C.: Origin, importance, and predictive limits of internal climate
425 variability, *Environ. Res. Clim.*, 2, 023001, <https://doi.org/10.1088/2752-5295/accf30>,
426 2023.
- 427 Lorenz, E. N.: Deterministic Nonperiodic Flow, *J. Atmospheric Sci.*, 20, 130–141,
428 [https://doi.org/10.1175/1520-0469\(1963\)020%253C0130:DNF%253E2.0.CO;2](https://doi.org/10.1175/1520-0469(1963)020%253C0130:DNF%253E2.0.CO;2),
429 1963.
- 430 Maher, N., Milinski, S., Suarez-Gutierrez, L., Botzet, M., Dobrynin, M., Kornblueh, L.,
431 Kröger, J., Takano, Y., Ghosh, R., Hedemann, C., Li, C., Li, H., Manzini, E., Notz, D.,
432 Putrasahan, D., Boysen, L., Claussen, M., Ilyina, T., Olonscheck, D., Raddatz, T.,
433 Stevens, B., and Marotzke, J.: The Max Planck Institute Grand Ensemble: Enabling
434 the Exploration of Climate System Variability, *J. Adv. Model. Earth Syst.*, 11, 2050–
435 2069, <https://doi.org/10.1029/2019MS001639>, 2019.
- 436 Mann, M. E., Steinman, B. A., and Miller, S. K.: Absence of internal multidecadal and
437 interdecadal oscillations in climate model simulations, *Nat. Commun.*, 11, 49,
438 <https://doi.org/10.1038/s41467-019-13823-w>, 2020.



- 439 Mann, M. E., Steinman, B. A., Brouillette, D. J., and Miller, S. K.: Multidecadal climate
440 oscillations during the past millennium driven by volcanic forcing, *Science*, 371, 1014–
441 1019, <https://doi.org/10.1126/science.abc5810>, 2021.
- 442 Murphy, L. N., Bellomo, K., Cane, M., and Clement, A.: The role of historical forcings
443 in simulating the observed Atlantic multidecadal oscillation, *Geophys. Res. Lett.*, 44,
444 2472–2480, <https://doi.org/10.1002/2016GL071337>, 2017.
- 445 Osborn, T. J. and Kennedy, J. J.: Revised historical record sharpens perspective on
446 global warming, *Nature*, 635, 560–561, <https://doi.org/10.1038/d41586-024-03551-7>,
447 2024.
- 448 Otterå, O. H., Bentsen, M., Drange, H., and Suo, L.: External forcing as a metronome
449 for Atlantic multidecadal variability, *Nat. Geosci.*, 3, 688–694,
450 <https://doi.org/10.1038/ngeo955>, 2010.
- 451 Peings, Y., Simpkins, G., and Magnusdottir, G.: Multidecadal fluctuations of the North
452 Atlantic Ocean and feedback on the winter climate in CMIP5 control simulations, *J.*
453 *Geophys. Res. Atmospheres*, 121, 2571–2592,
454 <https://doi.org/10.1002/2015JD024107>, 2016.
- 455 Robson, J., Menary, M. B., Sutton, R. T., Mecking, J., Gregory, J. M., Jones, C., Sinha,
456 B., Stevens, D. P., and Wilcox, L. J.: The Role of Anthropogenic Aerosol Forcing in
457 the 1850–1985 Strengthening of the AMOC in CMIP6 Historical Simulations, *J. Clim.*,
458 35, 6843–6863, <https://doi.org/10.1175/JCLI-D-22-0124.1>, 2022.
- 459 Robson, J., Sutton, R., Menary, M. B., and Lai, M. W. K.: Contrasting internally and
460 externally generated Atlantic Multidecadal Variability and the role for AMOC in CMIP6
461 historical simulations, *Philos. Trans. R. Soc. Math. Phys. Eng. Sci.*, 381, 20220194,
462 <https://doi.org/10.1098/rsta.2022.0194>, 2023.
- 463 Rodgers, K. B., Lee, S.-S., Rosenbloom, N., Timmermann, A., Danabasoglu, G.,
464 Deser, C., Edwards, J., Kim, J.-E., Simpson, I. R., Stein, K., Stuecker, M. F.,
465 Yamaguchi, R., Bódai, T., Chung, E.-S., Huang, L., Kim, W. M., Lamarque, J.-F.,
466 Lombardozzi, D. L., Wieder, W. R., and Yeager, S. G.: Ubiquity of human-induced
467 changes in climate variability, *Earth Syst. Dyn.*, 12, 1393–1411,
468 <https://doi.org/10.5194/esd-12-1393-2021>, 2021.
- 469 Shiogama, H., Tatebe, H., Hayashi, M., Abe, M., Arai, M., Koyama, H., Imada, Y.,
470 Kosaka, Y., Ogura, T., and Watanabe, M.: MIROC6 Large Ensemble (MIROC6-LE):
471 experimental design and initial analyses, *Earth Syst. Dyn.*, 14, 1107–1124,
472 <https://doi.org/10.5194/esd-14-1107-2023>, 2023.
- 473 Si, D. and Hu, A.: Internally Generated and Externally Forced Multidecadal Oceanic
474 Modes and Their Influence on the Summer Rainfall over East Asia, *J. Clim.*, 30, 8299–
475 8316, <https://doi.org/10.1175/JCLI-D-17-0065.1>, 2017a.
- 476 Si, D. and Hu, A.: Internally Generated and Externally Forced Multidecadal Oceanic
477 Modes and Their Influence on the Summer Rainfall over East Asia, *J. Clim.*, 30, 8299–
478 8316, <https://doi.org/10.1175/JCLI-D-17-0065.1>, 2017b.



- 479 Simpson, I. R., Rosenbloom, N., Danabasoglu, G., Deser, C., Yeager, S. G.,
480 McCluskey, C. S., Yamaguchi, R., Lamarque, J.-F., Tilmes, S., Mills, M. J., and
481 Rodgers, K. B.: The CESM2 Single-Forcing Large Ensemble and Comparison to
482 CESM1: Implications for Experimental Design, *J. Clim.*, 36, 5687–5711,
483 <https://doi.org/10.1175/JCLI-D-22-0666.1>, 2023.
- 484 Sippel, S., Kent, E. C., Meinshausen, N., Chan, D., Kadow, C., Neukom, R., Fischer,
485 E. M., Humphrey, V., Rohde, R., de Vries, I., and Knutti, R.: Early-twentieth-century
486 cold bias in ocean surface temperature observations, *Nature*, 635, 618–624,
487 <https://doi.org/10.1038/s41586-024-08230-1>, 2024.
- 488 Sutton, R. T. and Dong, B.: Atlantic Ocean influence on a shift in European climate in
489 the 1990s, *Nat. Geosci.*, 5, 788–792, <https://doi.org/10.1038/ngeo1595>, 2012.
- 490 Sutton, R. T. and Hodson, D. L. R.: Atlantic Ocean Forcing of North American and
491 European Summer Climate, *Science*, 309, 115–118,
492 <https://doi.org/10.1126/science.1109496>, 2005.
- 493 Swart, N. C., Cole, J. N. S., Khari, V. V., Lazare, M., Scinocca, J. F., Gillett, N. P.,
494 Anstey, J., Arora, V., Christian, J. R., Hanna, S., Jiao, Y., Lee, W. G., Majaess, F.,
495 Saenko, O. A., Seiler, C., Seinen, C., Shao, A., Sigmond, M., Solheim, L., von Salzen,
496 K., Yang, D., and Winter, B.: The Canadian Earth System Model version 5
497 (CanESM5.0.3), *Geosci. Model Dev.*, 12, 4823–4873, <https://doi.org/10.5194/gmd-12-4823-2019>, 2019.
- 499 Taylor, K. E., Stouffer, R. J., and Meehl, G. A.: An Overview of CMIP5 and the
500 Experiment Design, *Bull. Am. Meteorol. Soc.*, 93, 485–498,
501 <https://doi.org/10.1175/BAMS-D-11-00094.1>, 2012.
- 502 Wang, C. and Zhang, L.: Multidecadal Ocean Temperature and Salinity Variability in
503 the Tropical North Atlantic: Linking with the AMO, AMOC, and Subtropical Cell, *J.*
504 *Clim.*, 26, 6137–6162, <https://doi.org/10.1175/JCLI-D-12-00721.1>, 2013.
- 505 Williams, K. D., Copsey, D., Blockley, E. W., Bodas-Salcedo, A., Calvert, D., Comer,
506 R., Davis, P., Graham, T., Hewitt, H. T., Hill, R., Hyder, P., Ineson, S., Johns, T. C.,
507 Keen, A. B., Lee, R. W., Megann, A., Milton, S. F., Rae, J. G. L., Roberts, M. J., Scaife,
508 A. A., Schiemann, R., Storkey, D., Thorpe, L., Watterson, I. G., Walters, D. N., West,
509 A., Wood, R. A., Woollings, T., and Xavier, P. K.: The Met Office Global Coupled Model
510 3.0 and 3.1 (GC3.0 and GC3.1) Configurations, *J. Adv. Model. Earth Syst.*, 10, 357–
511 380, <https://doi.org/10.1002/2017MS001115>, 2018.
- 512 Wills, R. C. J., Armour, K. C., Battisti, D. S., and Hartmann, D. L.: Ocean–Atmosphere
513 Dynamical Coupling Fundamental to the Atlantic Multidecadal Oscillation, *J. Clim.*, 32,
514 251–272, <https://doi.org/10.1175/JCLI-D-18-0269.1>, 2019.
- 515 Zhang, R., Sutton, R., Danabasoglu, G., Kwon, Y.-O., Marsh, R., Yeager, S. G.,
516 Amrhein, D. E., and Little, C. M.: A Review of the Role of the Atlantic Meridional
517 Overturning Circulation in Atlantic Multidecadal Variability and Associated Climate
518 Impacts, *Rev. Geophys.*, 57, 316–375, <https://doi.org/10.1029/2019RG000644>, 2019.

<https://doi.org/10.5194/egusphere-2026-699>
Preprint. Discussion started: 27 February 2026
© Author(s) 2026. CC BY 4.0 License.



519 Zhao, B., Lin, P., Chen, X. & Wei, J. FGOALS-g3 Super-large ensemble simulation
520 (V3). <https://doi.org/10.11922/sciencedb.01332>, 2023.



521 Acknowledgement

522 This publication has emanated from research conducted with the financial support of
523 Research Ireland, Northern Ireland's Department of Agriculture, Environment and
524 Rural Affairs (DAERA), UK Research and Innovation (UKRI) via the International
525 Science Partnerships Fund (ISPF) under Grant number [22/CC/11103] at the Co-
526 Centre for Climate + Biodiversity + Water. We also receive philanthropic funding from
527 the Sunflower Charitable Foundation and the Fernhill Fund at Community Foundation
528 Ireland. Our Industry projects are part funded by our business partners. We are
529 grateful to the JASMIN platform and CANARI project for providing access to the
530 CANARI-LE model simulation outputs used in this study. We also acknowledge the
531 CESM2 Large Ensemble Community Project and supercomputing resources provided
532 by the IBS Center for Climate Physics in South Korea.

533

534 Financial support

535 This research is supported by Research Ireland, Northern Ireland's Department of
536 Agriculture, Environment and Rural Affairs (DAERA), UK Research and Innovation
537 (UKRI) via the International Science Partnerships Fund (ISPF) under Grant number
538 [22/CC/11103] at the Co-Centre for Climate + Biodiversity + Water.



539 Author contribution

540 Conceptualisation: YL, PT. Project administration: PT, EH. Funding acquisition: PT,
541 EH. Data curation: YL. Formal analysis: YL, PT. Investigation: YL, PT. Methodology:
542 YL, PT. Supervision: PT, EH. Visualisation: YL. Writing - original draft: YL. Writing -
543 review & editing: PT, EH, GM.

544

545 Competing interests

546 The authors declare no competing interests.